Internal disruptions and sawtooth like activity in LHD

J. Varela[1], L. Garcia[1], S. Ohdachi[2], K.Y. Watanabe[2]

[1] *Universidad Carlos III, 28911 Leganés, Madrid, Spain*

[2] *National Institute for Fusion Science, Oroshi-cho 322-6, Toki 509-5292, Japan*

Introduction. Sawtooth like activity is observed in LHD operation for inward configurations [1]. This activity was detected in pellet fuelled plasmas with peaked pressure profiles and intense NBI heating with and without large net toroidal current. There is no experimental evidence of internal disruptions but these events can be driven in future operation with high beta and plasma density in inward configurations and it is important to foresee its effects on plasma confinement.

The aim of the present research is to simulate sawtooth like activity and internal disruptions in order to improve the understanding of these relaxation events. The simulations were performed using the FAR-3D code. This code solves the set of reduced non-linear resistive MHD equations to study the evolution of a perturbed VMEC equilibrium without net toroidal current before a sawtooth like event observed during a experiment in LHD.

Figure 1 (a) shows the pressure and rotational transform profiles for the equilibrium. It corresponds to a configuration with high magnetic field, inward-shifted, and moderate beta value.

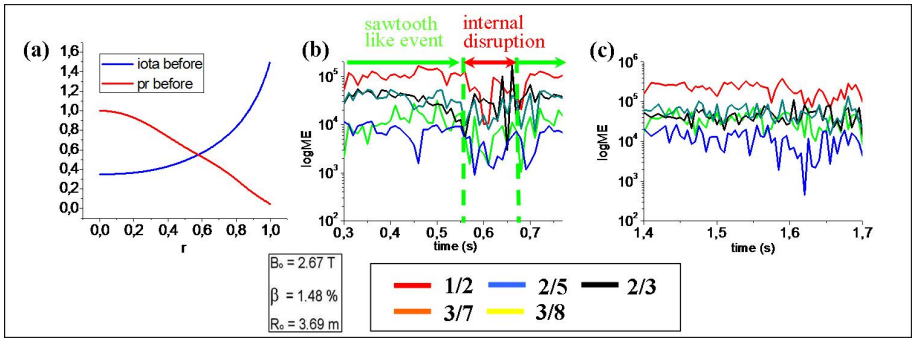

Figure 1: (a) Pressure and rotational transform profiles. Magnetic energy evolution of the dominant modes: (b) $\beta_0 = 1.2$-1.34% and (c) $\beta_0 = 1.48\%$.

MHD Equation and numerical scheme. The system behaviour is determined by the evolution of the poloidal magnetic flux ψ, the vorticity U and the pressure p. There is not averaging in the toroidal angle and a full 3D equilibria is used. The magnetic and velocity fields are expressed as $\vec{v} = \sqrt{g}\vec{\nabla}\zeta \wedge \vec{\nabla}\phi$ and $\vec{B} = \vec{\nabla}\zeta \wedge \vec{\nabla}\psi$, where ϕ is a stream function proportional to the electrostatic potential, and ζ is the toroidal angle. We use Boozer coordinates (ρ, θ, ζ), where θ is the poloidal angle, and ρ is the radial coordinate proportional to the square root of the toroidal flux (normalized to unity in the boundary). All functions have equilibrium and dy-

namic components like $A = A_{eq} + \tilde{A}$ and $A_{eq} >> \tilde{A}$. The set of dimensionless reduced equations is

$$\frac{\partial \tilde{\psi}}{\partial t} = \nabla_{||}\Phi + \eta \tilde{J}_{\zeta}$$

$$\frac{\partial U}{\partial t} = -\vec{v}\cdot\vec{\nabla}U + S^2\left[\frac{\beta_0}{2\varepsilon^2}\left(\frac{1}{\rho}\frac{\partial\sqrt{g}}{\partial\theta}\frac{\partial\tilde{p}}{\partial\rho} - \frac{\partial\sqrt{g}}{\partial\rho}\frac{1}{\rho}\frac{\partial\tilde{p}}{\partial\theta}\right) + \nabla_{||}J^{\zeta}\right]$$

$$\frac{\partial p}{\partial t} = -\vec{v}\cdot\vec{\nabla}p$$

where the vorticity is $U = \sqrt{g}\left[\vec{\nabla}\times\sqrt{g}\vec{v}\right]^{\zeta}$, and η is the resistivity. $S = \tau_R/\tau_{hp}$ is the magnetic Reynolds number, where $\tau_R = \mu_0 a^2/\eta_0$ is the resistive time, and $\tau_{hp} = R_0(\mu_0\rho_m)^{1/2}/B_0$ is the Alfvén poloidal time. J_{ζ} is the toroidal component of the current density, $\varepsilon = a/R_0$ is the inverse aspect ratio, $\sqrt{g}$ is the Jacobian of the coordinates transformation and ρ_m is the mass density. The $\nabla_{||}$ operator indicates derivative along the magnetic field line, and is defined as $\nabla_{||} = \frac{\partial}{\partial\zeta} + \iota\frac{\partial}{\partial\theta} - \frac{1}{\rho}\frac{\partial\tilde{\psi}}{\partial\theta}\frac{\partial}{\partial\rho} + \frac{\partial\tilde{\psi}}{\partial\rho}\frac{1}{\rho}\frac{\partial}{\partial\theta}$. All the lengths in the code are normalized to the minor radius a, the resistivity and pressure to their value in the magnetic axis and the time to the resistive time.

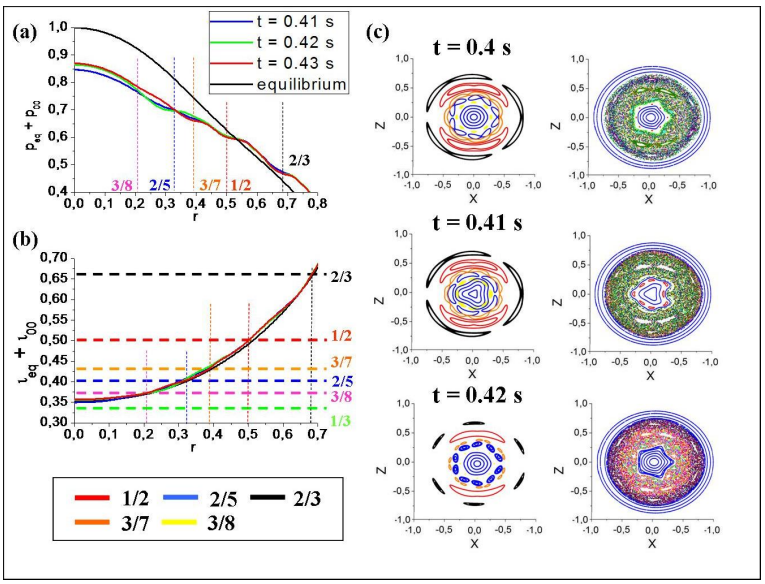

Figure 2: (a) Pressure and (b) iota profile. (c) Dominant helicities and Poincaré plots. Non resonant sawtooth.

Simulation results. The magnetic energy evolution of the dominant modes is shown in Fig. 1 (b) for $\beta_0 = 1.2 - 1.34\%$, and in Fig. 1 (c) for $\beta_0 = 1.48\%$. In figure 1 (b) two different oscillating events are observed, the first is a non resonant sawtooth like event, and the second is an internal disruption at the rational surface $n/m = 1/2$. Sawtooth like events are related with fast changes in the dominant modes energy $1/2$, $2/3$ and a magnetic energy local maximum of

mode $1/3$. Internal disruptions are preceded by a fast decrease of the dominant modes energy before a sharply increase of modes $2/3$ and $2/5$ energy, with a local minimum of the $1/3$ mode energy. In figure 1 (c) the internal disruption is not observed but there is a new oscillation that we call resonant sawtooth like event.

Non resonant sawtooth. At $t = 0.41$ s, figure 2 (a), the pressure profile flattening in the inner region is driven by the mode $2/5$, in the middle region by the modes $1/2$ and $3/7$ and in the periphery by the mode $2/3$. The magnetic islands corresponding to the dominant helicities and the Poincaré plots obtained including all the Fourier components are shown in Fig. 2 (c), at $t = 0.40$ and $t = 0.41$ s. Magnetic islands $1/2$, $2/5$, $3/7$ and $3/8$ are overlapped between the middle and inner region and a stochastic field region appears. The non resonant effect of the mode $1/3$ over the plasma is the main destabilizing contribution between the inner and middle plasma region, Fig. 2 (b). If the maximum energy of mode $1/3$ is reached, and the iota profile is near $\iota = 1/3$ value, a non resonant sawtooth like event can be driven between the middle and inner plasma region.

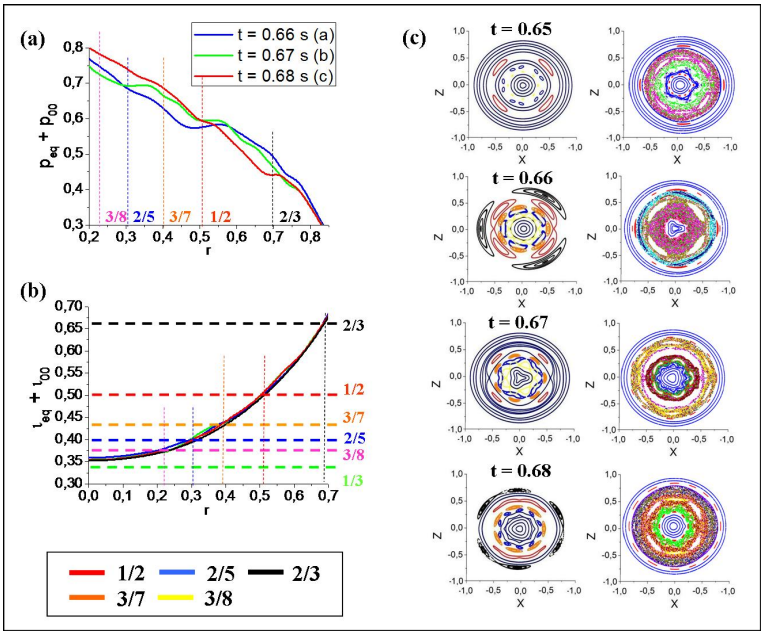

Figure 3: (a) Pressure and (b) iota profile. (c) Dominant helicities and Poincaré plots. Internal disruption.

Internal disruption. At $t = 0.66$ s there is a strong deformation in $\rho = 0.5$ driven by the rational surface $1/2$, figure 3 (a) and (b). The effect of other rational surfaces along the plasma is negligible. At $t = 0.67$ s the flattening of the profile in the middle region decreases and a new profile flattening at $\rho = 0.3$ driven by the rational surface $2/5$ appears, but these deformations are not overlapped. At $t = 0.68$ s the profile flattening disappears in the inner region and

decreases in the middle plasma, while in the periphery the deformation driven by the rational surface $2/3$ is large. At $t = 0.65$ s the islands' size is small and there is not a strong overlapping, Fig. 3(c). At $t = 0.66$ s there are broad magnetic islands of different helical families overlapped between the inner and the periphery plasma region, with the island $1/2$ and $2/3$ the largest ones. A stochastic region appears along the plasma. At $t = 0.67$ s the magnetic reconnection takes place in the periphery and middle plasma, while the islands overlapping is still large in the inner region and the magnetic surface deformation close to the magnetic axis is strong. At $t = 0.68$ s the magnetic reconnection reaches the plasma inner region.

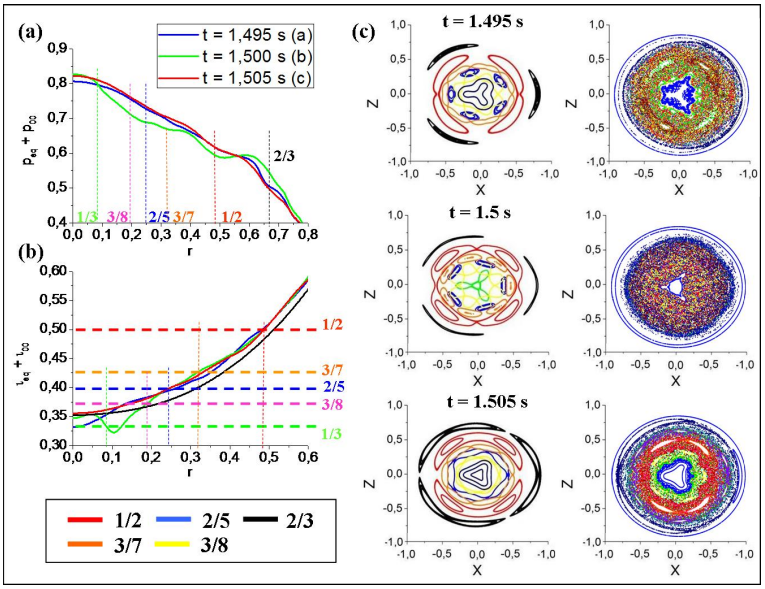

Figure 4: (a) Pressure and (b) iota profile. (c) Dominant helicities and Poincaré plots. Resonant sawtooth.

Resonant sawtooth. At $t = 1.495$ and 1.505 s the largest perturbations are driven by the rational surfaces $1/2$ and $2/3$, Figs. 4 (a) and (b). At $t = 1.5$ s the rational surface $1/3$ is located close to the magnetic axis around $\rho = 0.1$. The pressure profile deformation in the inner plasma is not overlapped with the $1/2$ rational surface perturbation around $\rho = 0.48$. At $t = 1.5$ s the resonant mode $1/3$ drives a strong magnetic surface deformation near the magnetic axis, and $1/3$ islands appear, Fig. 4 (c). The islands $1/3$ are overlapped with $2/5$, $3/8$, $3/7$ and $1/2$ islands between the inner and middle plasma, and the stochastic region reach the plasma core.

References

[1] OHDACHI, S. ET AL. 21 IAEA FUSION ENERGY CONFERENCE , EX/P8-15, 2006.